Novel Mesoporous Solid Superacidic Catalysts: Activity and Selectivity in the Synthesis of Thymol by Isopropylation of *m*-Cresol with 2-Propanol over UDCaT-4, -5, and -6

Ganapati D. Yadav* and Ganesh S. Pathre

Department of Chemical Engineering, University Institute of Chemical Technology (UICT), University of Mumbai, Matunga, Mumbai - 400 019, India

Received: May 5, 2005; In Final Form: August 26, 2005

The alkylation of *m*-cresol with isopropyl alcohol in the presence of novel superacidic catalysts named as UDCaT-4, UDCaT-5, and UDCaT-6 was investigated. The catalysts are modified versions of zirconia showing high catalytic activity, stability, and reusability in the presence of water as compared to conventional sulfated zirconia. The objective of the present investigation was to explore the potential of these catalysts in this alkylation of *m*-cresol with isopropyl alcohol to thymol, which has widescale applications. The reactions were conducted in liquid phase in the temperature range of 433−473 K. Both, O- and C-alkylated products were obtained at lower temperatures, while at higher temperatures, thymol was the main product of the reaction. The catalytic activity increases in the order UDCaT-5 > UDCaT-6 >UDCaT-4 > sulfated zirconia. Thymol could be efficiently obtained with selectivity reaching up to 79% at an isopropyl alcohol conversion of 92% with UDCaT-5. This process can be a replacement for the existing process based on zeolites where high temperature and pressure are required. Synergistic effects of very high sulfur content present (9% S) and preservation of the tetragonal phase in UDCaT-5, in comparison with sulfated zirconia (4% S), were responsible for higher catalytic activity. A systematic investigation of the effects of various operating parameters was accomplished, and a mathematical model is developed to describe the reaction pathway and validated with experimental results. The reaction was carried out without using solvent, and the process subscribes to the principles of green chemistry.

1. Introduction

Friedel−Crafts alkylation and acylation reactions are practiced in a number of industries and involve use of a variety of acid catalysts. Some of the well-established processes still employ homogeneous acid catalysts in batch reactors using a large excess of the substrate or solvent causing problems of corrosion, pollution, loss of selectivity of the desired product, etc. The catalysts $AlCl_3$, BF_3, $TiCl_4$, H_2SO_4, and HF and solvents such as nitrobenzene, CS_2, and halocarbons are used rampantly. A relatively high concentration of catalyst is needed; often the amounts are more than stoichiometric, making the reactions inherently polluting.[1−3] Amid increasing societal, environmental, and economic pressure, efforts are devoted to the development of environmentally friendly catalysts for the production of industrially important chemicals and chemical intermediates.[4−6]

Several isopropylation products of cresols are used industrially. However, isopropylation of *m*-cresol continues to attract considerable attention, because one of the alkylation products, thymol, leads to menthol on hydrogenation.[7−9] Menthol has a characteristic peppermint odor and is used as a raw material for the production of antiseptic, local anesthetic, antibacterial and antifungal agents, flavors, fragrances, and preservatives.[10,11] Thymol as such exhibits activity in protecting low-density lipoproteins and also as an antioxidant.[12,13] It also plays an important role as intermediate in perfumery. Isopropylation of *m*-cresol has been studied with various alkylating agents such as propylene, isopropyl alcohol (IPA), isopropyl bromide, etc. Alkylation of *m*-cresol with isopropyl alcohol has already been reported over oxide catalysts[14] and calcined Mg−Al hydrotalcites[15] and with propylene over acidic catalysts.[16] Activated alumina,[17] γ-Al_2O_3,[18] Al $(OC_6H_5)_3$, and $ZnCl_2$−HCl[10] have been used as catalysts in the liquid-phase alkylation of *m*-cresol. Y-type zeolites, ZSM-5, erionite, and mordenite[19] and supported metal sulfates[7] were used in vapor-phase reactions, and harsh conditions were required because the acidity of zeolites is less. Further there was a problem due to formation of undesired products using these catalysts reducing selectivity for thymol. In an industrial process employed by Bayer AG, thymol is obtained by liquid-phase isopropylation of *m*-cresol with propylene in the presence of activated alumina at 633 K and at a pressure of 50 atm.[20] The need for high temperature and pressure for these processes is the major drawback. Also the use of propylene is associated with coke formation due to its oligomerization, which results in deactivation of the catalyst and loss of propylene. Besides, due to the problems associated with unavailability, cost, transportation, and handling of propylene, it is advantageous to generate propylene in-situ. Dehydration of isopropyl alcohol (IPA) is an attractive source to produce propylene in-situ. IPA dehydration leads to the formation of propylene and water. This water, formed in-situ, suppresses coke formation and results in prolonged catalytic activity. When excess IPA is present in the reaction mixture, IPA further reacts with propylene to form diisopropyl ether (DIPE), which itself is an excellent alkylating agent as compared to IPA.[22]

Alcohol dehydration on solid acids is one of the most extensively studied catalytic reactions, to study both reaction mechanisms and catalyst active sites. The dehydration of alcohols is highly temperature sensitive, and depending on the type of alcohol and catalyst, it presents different kinetic behavior. Many reviews on alcohol dehydration, mainly on alumina, have been published.[23] Balaceanu and Jungers,[24] studying the kinetics of methanol (MeOH) dehydration over Al_2O_3, concluded that a

* Tel: +91-22-2410 2121, +91-22-2414 5616 ext 291. Fax: +91-22-2410 2121, +91-22-2414 5614. E-mail: gdyadav@yahoo.com, gdyadav@udct.org.

10.1021/jp052335e CCC: $30.25
Published on Web 11/11/2005

second-order reaction mechanism between two adsorbed MeOH molecules explains the experimental data. Knözinger and Kallo,[25] while studying MeOH and ethanol (EtOH) dehydration to ether over Al_2O_3, stated that the adsorption of the two reactant molecules occurs on different active sites, an acidic and a basic site. By this mechanism, ether formation takes place by the surface reaction between the adsorbed alcohol molecule on an acidic site and an adsorbed alkoxide anion on a basic site. Jain and Pillai[26] proposed a similar reaction mechanism for dehydration of the same alcohols to ether. Experimental evidence demonstrated that primary and secondary alcohols are dehydrated to yield ether by a concerted mechanism, E2, involving both the acidic and the basic sites of Al_2O_3.[27] It was also demonstrated that alcohol dehydration to yield olefins is catalyzed by solid acids.[23,28] It has been pointed out that the basic properties of some oxides also play an important role in these dehydration reactions. The studies by Golay et al.[29] on ethanol dehydration on γ-alumina at 180 °C and 140 kPa where both acidic and basic sites are present show a second-order equation. Luy and Parera[30] have studied the dehydration of alcohols on Al_2O_3, $SiO_2-Al_2O_3$, TiO_2-MgO, $ZnO-Al_2O_3$, and Rb−Mn exchanged zeolites with different acid−base relations as catalysts for dehydration of methanol and isopropyl alcohol. Catalytic activity is always correlated with surface acidity not only for olefin formation (El mechanism) but also for ether formation, even when the latter reaction proceeds through an E2 acid−base mechanism.[28,30]

Thus, it is apparent that there still exists a scope to develop better catalysts that would catalyze the isopropylation of *m*-cresol with excellent conversion and selectivity at comparatively low temperatures, with ease of preparation, and having good reusability and stability in the presence of water. The use of mesoporous materials as catalysts has been growing for the past decade. Hexagonal mesoporous silica (HMS) is frequently used as the material to incorporate catalytic sites. Our attempts to generate solid superacids in mesoporous materials resulted into new materials called UDCaT-4, -5, and -6. The work deals with the alkylation of *m*-cresol with isopropyl alcohol to produce thymol by using a new breed of superacidic mesoporous materials, including the kinetic modeling.

2. Experimental Section

2.1. Chemicals. Isopropyl alcohol (IPA) and *m*-cresol were procured from E. Merck (India) Ltd., Mumbai. Zirconium oxychloride, aluminum nitrate, ammonium persulfate (AR grade), and aqueous ammonia solution were obtained from M/s. s. d. fine Chemicals Ltd., Mumbai. Hexadecylamine and chlorosulfonic acid were purchased from Spectrochem Ltd., Mumbai, India. Tetraethyl orthosilicate (TEOS) was obtained from Fluka, Germany.

2.2. Catalyst Preparation and Characterization. *2.2.1. Catalyst Preparation.* 2.2.1.1. Preparation of Sulfated Zirconia. Sulfated zirconia was prepared by adding aqueous ammonia solution to zirconium oxychloride solution at a pH of 10, as detailed elsewhere.[21,31] The precipitate was thoroughly washed with distilled water and made free from ammonia and chloride ions. It was dried in an oven at 120 °C for 24 h. The sulfation of the zirconia was done using 15 mL g^{-1} of 0.5 M sulfuric acid. It was dried at 110 °C and calcined at 650 °C for 3 h.

2.2.1.2. Preparation of UDCaT-4. The ordered hexagonal mesoporous silica (HMS) was prepared according to our earlier work.[32] Desired quantities of zirconium oxychloride and aluminum nitrate were dissolved in aqueous solution and added to precalcined HMS by the incipient wetness technique. After addition, the solid was dried in an oven at 110 °C for 3 h. The dried material was hydrolyzed by ammonia gas and washed with deionized water until a neutral filtrate was obtained, and the absence of chlorine ion in the filtrate was detected by phenolphthalein and silver nitrate tests. It was then dried in an oven for 24 h at 110 °C. Persulfation was carried out by immersing the above solid material in a 0.5 M aqueous solution of ammonium persulfate for 30 min. It was dried at 110 °C for 24 h and calcined at 650 °C for 3 h to get active catalyst called UDCaT-4 with 0.6% w/w of alumina.[33]

2.2.1.3. Preparation of UDCaT-5. UDCaT-5 was prepared by adding aqueous ammonia solution to zirconium oxychloride ($ZrOCl_2 \cdot 8H_2O$) solution at pH of 9−10. The precipitated zirconium hydroxide so obtained was washed with deionized water until a neutral filtrate was obtained. The absence of chlorine ion was detected by the $AgNO_3$ test. A material balance on chloride ions before and after precipitation and washing shows no retention of Cl^- on the solid. Zirconium hydroxide was dried in an oven for 24 h at 100 °C and was crushed to 100 mesh size. $Zr(OH)_4$ then immersed in 15 cm^3 g^{-1} of 0.5 M solution of chlorosulfonic acid and ethylene dichloride. All materials were immersed for 5 min in the solution and then without allowing moisture absorption were kept in an oven, and the heating was started slowly to 120 °C after about 30 min. These materials were kept in oven at 120 °C for 24 h and calcined at 650 °C for 3 h to get the active catalyst UDCaT-5.[34]

2.2.1.4. Preparation of UDCaT-6. UDCaT-6 was prepared by adding an aqueous solution of 2.5 g of zirconium oxychloride to 5 g of precalcined HMS by the incipient wetness technique, and it was dried in an oven at 120 °C for 3 h. The dried material was hydrolyzed by ammonia gas and washed with distilled water until no chloride ions were detected, which was confirmed by the $AgNO_3$ test. It was further dried in an oven for 2 h at 120 °C. $Zr(OH)_4$/HMS was immersed in 15 cm^3 g^{-1} of 0.5 M chlorosulfonic acid in ethylene dichloride. It was soaked for 5 min in the solution, and then without allowing moisture absorption, it was oven dried to evaporate the solvent at 120 °C after about 30 min. The sample was kept in the oven at 120 °C for further 24 h and calcined thereafter at 650 °C for 3 h to get the active catalyst UDCaT-6.[35]

2.2.2. Characterization of Catalysts. UDCaT-4,[33] UDCaT-5,[34] and UDCaT-6[35] were completely characterized by X-ray diffraction (XRD), BET surface area, and Fourier transform infrared spectroscopy (FTIR), and the details were published recently by us. Only a few salient features, which are thought to be important, are reported here.

2.2.2.1. Characterization of UDCaT-4. The XRD, BET surface area, and pore size analyses provided an explanation for the entrapment of nanoparticles of persulfated alumina zirconia (PAZ) (<3.6 nm) in mesoporous of HMS. The XRD of UDCaT-4 suggested that the structural integrity of HMS was maintained even after converting it into UDCaT-4. The diffractogram of UDCaT-4 further revealed that the introduction of a small amount of alumina (0.16% w/w) and sulfate ion (1.17% w/w) stabilized the tetragonal phase of the zirconia, which is an ideal phase conducive for superacidity in sulfated zirconia, into the pores of HMS. Furthermore, the pore volume of UDCaT-4 (0.21 cm^3 g^{-1}) is much less than that of pure HMS (0.78 cm^3 g^{-1}) indicating that a large amount of crystalline zirconia (9.01% w/w) and alumina must be present inside pores of UDCaT-4. FTIR spectroscopy and energy dispersive analysis of X-rays (EDAX) further support the assumption drawn on introduction of sulfate ion in UDCaT-4. The sulfur Ka_1 and zirconium La_1 distribution spectra determined by EDAX analysis

show the incorporation and homogeneous distribution of zirconia and sulfur atoms in UDCaT-4.

The TPD profiles of PAZ and UDCaT-4 show that although UDCaT-4 possesses both weak and medium acid sites, the total acid sites of UDCaT-4 (0.56 mmol g^{-1}) are greater than those of PAZ (0.09 mmol g^{-1}).[32,33]

The SEM of UDCaT-4 revealed that similar to the morphology of HMS, UDCat-4 is made up of submicrometer-sized free-standing or aggregated sphere-shaped particles. SEM analysis further supports the argument that active centers of the PAZ are successfully embedded in HMS and the structural integrity of HMS is unaltered even after it is converted to UDCaT-4.

2.2.2.2. Characterization of UDCaT-5. Ammonia-TPD was used to determine the acid strength of UDCaT-5. It shows that apart from intermediate and strong acidic sites present in sulfated zirconia, UDCaT-5 also contains superacidic sites. Elemental analysis shown that UDCaT-5 contains 9% sulfate content, which is the highest reported so far in the literature. IR spectroscopy confirms that the chlorosulfonic acid is decomposed during calcination at 650 °C and sulfate ions are retained on the surface of UDCaT-5, and thus the sulfur content is higher in UDCaT-5. The XRD study proved that the tetragonal phase in the UDCaT-5 was preserved. BET surface area and pore size analysis showed that the surface area of UDCaT-5 decreased abruptly at the maximum sulfur content. This was due to the migration of sulfate ions from the bulk phase to the zirconia matrix. Thus maximum sulfur present on a surface decreases its surface area. Thus, UDCaT-5 is superacidic due to the presence of a very high sulfur content and preservation of tetragonal phase of zirconia.

2.2.2.3. Characterization of UDCaT-6. FTIR spectroscopy and EDAX analyses support the introduction and retension of sulfate ion in UDCaT-6. XRD, BET surface area, and pore size analysis provided an explanation for entrapment of nanoparticles of zirconia in mesoporous of HMS. The XRD of UDCaT-6 suggested that the structural integrity of HMS was retained even after converting it into UDCaT-6. Furthermore, the pore volume of UDCaT-6 (0.7 cm^3 g^{-1}) is much less than that of pure HMS (1.2 cm^3 g^{-1}) indicating that large amount of crystalline nanoparticles of zirconia must be present inside the pores of UDCaT-6. The sulfur Ka_1 and zirconium La_1 distribution spectra determined by EDAX analysis show the incorporation and homogeneous distribution of zirconia and sulfur atoms in UDCaT-6. The SEM of UDCaT-6 revealed that similar to the morphology of HMS, UDCaT-6 is made up of submicrometer-sized free-standing or aggregated sphere-shaped particles and that active centers of zirconia are successfully embedded in HMS and the structural integrity of HMS is unaltered even after it is converted to UDCaT-6.

2.3. Apparatus and Procedures. All experiments were carried out in a 100 cm^3 stainless steel Parr autoclave. A four bladed pitched turbine impeller was used for agitation. The temperature was maintained at ±1 °C of the desired value. Known quantities of reactants and catalyst were charged into the autoclave, the temperature was raised to the desired value, and agitation was started. Then, an initial sample was withdrawn. Further samples were drawn at periodic intervals up to 2 h. A standard experiment consisted of 0.33 mol of *m*-cresol, 0.066 mol of IPA, and a catalyst loading of 0.05 g cm^{-3} of total volume of liquid. The temperature was maintained at 180 °C and the speed of agitation at 1000 rpm under autogenous pressure. The reaction was carried out without any solvent. The total volume of liquid phase was 35 cm^3. Propylene formed in-situ was not allowed to escape the reaction vessel.

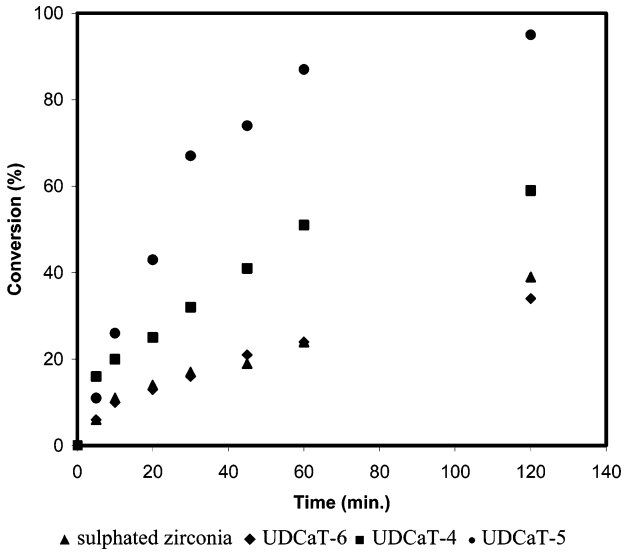

Figure 1. Effect of various catalysts: *m*-cresol = 0.33 mol; IPA = 0.066 mol; catalyst loading = 0.05 g cm^{-3}; temperature = 200 °C; speed of agitation = 1000 rpm; total volume = 35 cm^3.

2.4. Method of Analysis. Clear liquid samples were withdrawn at regular intervals by reducing the speed of agitation momentarily to zero and allowing the catalyst to settle to the bottom of the reactor. The samples were analyzed on a Chemito model 8510 GC equipped with a 10% OV-101 column (3.175 mm dia × 4 m length). A standard calibration method with synthetic mixtures was used for quantification of data. The reaction products were confirmed by GC-MS and authentic samples.

3. Result and Discussions

3.1. Choice of Catalysts. The activity and stability of UDCaT-4, UDCaT-5, and UDCaT-6 catalysts were tested by carrying out separate reactions, which produced HCl or water as the coproducts. Thus, benzylation of toluene with benzyl chloride and esterification *p*-cyclohexanol with acetic acid, where HCl and water are byproducts, respectively, were studied systematically, the details of which are given elsewhere.[32−35] The catalysts showed higher activity and good reusability as compared to sulfated zirconia. This indicated that the catalysts were stable in the presence of water and HCl. Moreover all catalysts were reusable in all these reactions without loss of activity. So it was thought desirable to investigate the efficacy of these catalysts in the liquid-phase isopropylation of *m*-cresol with isopropyl alcohol where water is one of the coproducts. Effects of various parameters such as effect of mole ratio, catalyst loading, and temperature on rates and product distribution are discussed to deduce the kinetics of the reaction.

3.2. Efficacies of Various Catalysts. The activities of UDCaT-4, UDCaT-5, UDCaT-6, and sulfated zirconia were evaluated. A 0.05 g cm^{-3} loading of catalyst based on the organic volume of the reaction mixture was employed at 200 °C and a speed of 1000 rpm. It was found that UDCaT-5 showed higher conversions compared to other catalysts, and the order of activity was UDCaT-5 > UDCaT-4 >UDCaT-6 > sulfated zirconia (Figure 1). All other catalysts contain fewer acidic sites compared to UDCaT-5, and thus the results are in order. UDCaT-5 also gave better reusability. Hence further experiments were conducted with UDCaT-5 due to its excellent activity, reusability, and stability. The concentration profile of several products is shown in Figure 2.

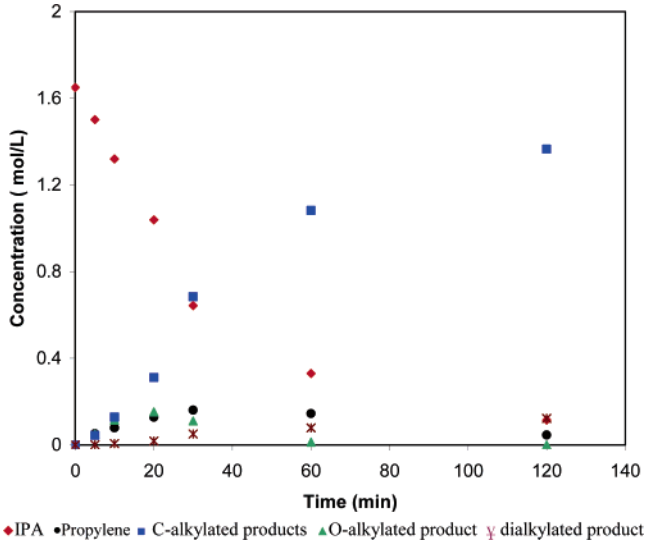

Figure 2. Concentration profile of various products in alkylation of *m*-cresol with IPA: *m*-cresol = 0.33 mol; IPA = 0.066 mol; UDCaT-5 = 0.05 g cm^{-3}; temperature = 180 °C; speed of agitation = 1000 rpm; total volume = 35 cm^3.

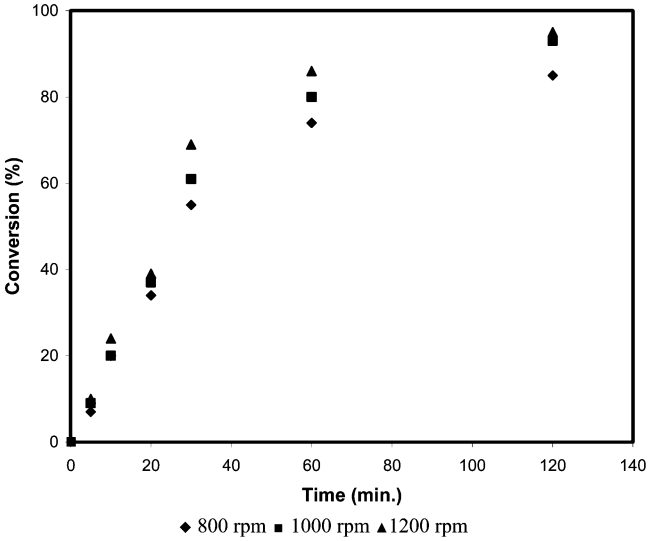

Figure 3. Effect of speed of agitation: *m*-cresol = 0.33 mol; IPA = 0.066 mol; UDCaT-5 = 0.05 g cm^{-3}; temperature = 180 °C; total volume = 35 cm^3.

3.3. Effect of Speed of Agitation. To assess the role of external mass transfer on the reaction rate, the effect of the speed of agitation (Figure 3) was studied. The speed of agitation was varied from 800 to 1200 rpm. It was observed that the conversion of isopropyl alcohol was practically the same in all the cases. The external mass transfer effects did not influence the reaction. Hence, all further reactions were carried out at 1000 rpm. The influence of external solid−liquid mass transfer resistance must be ascertained before a true kinetic model could be developed. Depending on the relative magnitudes of external resistance to mass transfer and reaction rates, different controlling mechanisms have been put forward.[36−40] This reaction is a typical solid−liquid slurry reaction involving the transfer of the limiting reactant IPA (A) and *m*-cresol (B) from the bulk liquidphase to the catalyst wherein external mass transfer of reactants to the surface of the catalyst particle, followed by intraparticle diffusion, adsorption, surface reactions, and desorption, takes place. Thus experimental and theoretical analyses were also done to establish that there was no effect of external mass transfer limitations.

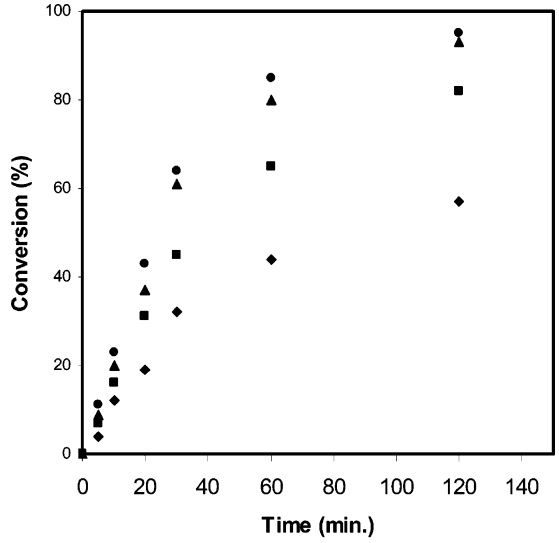

Figure 4. Effect of catalyst loading: *m*-cresol = 0.33 mol; IPA = 0.066 mol; speed of agitation = 1000 rpm; temperature = 180 °C; total volume = 35 cm^3.

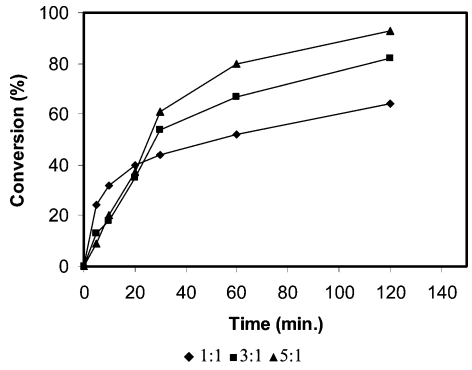

Figure 5. Effect of mole ratio *m*-cresol/IPA: UDCaT-5 = 0.05 g cm^{-3}; speed of agitation = 1000 rpm; temperature = 180 °C; total volume = 35 cm^3.

3.4. Effect of Catalyst Loading. The catalyst loading was varied over a range of 0.02−0.07 g cm^{-3} on the basis of total volume of the reaction mixture. Figure 4 shows the effect of catalyst loading on the conversion of *m*-cresol. The conversion increased with an increase in catalyst loading, which was due to the proportional increase in the number of active sites. However, beyond a catalyst loading of 0.05 g cm^{-3}, there was no significant increase in the conversion because the number of sites available were more than required, and hence all further experiments were carried out at 0.05 g cm^{-3}.

3.5. Proof of Absence of Intraparticle Resistance. A theoretical calculation was also done based on the Weitz−Prater criterion[41] to asses the influence of intraparticle diffusion resistance, according to which the value of $(-r_{obs}\rho_p R_p^2/(D_e[A_s])$ has to be far less than unity for the reaction to be intrinsically kinetically controlled. The calculated value of 2.203×10^{-3} further reveals the absence of mass transfer limitation at the reaction conditions.

3.6. Effect of Mole Ratio. The mole ratio of *m*-cresol to IPA was varied at 1:1, 3:1, and 5:1 (Figure 5) under otherwise similar operating conditions. As the mole ratio of *m*-cresol to IPA was increased, there was an increase in conversion of isopropyl alcohol with increase in selectivity for the C-alkylated product. At a shorter reaction times up to 20 min, the conversion for the 1:1 mole ratio was higher and it resulted in more formation of

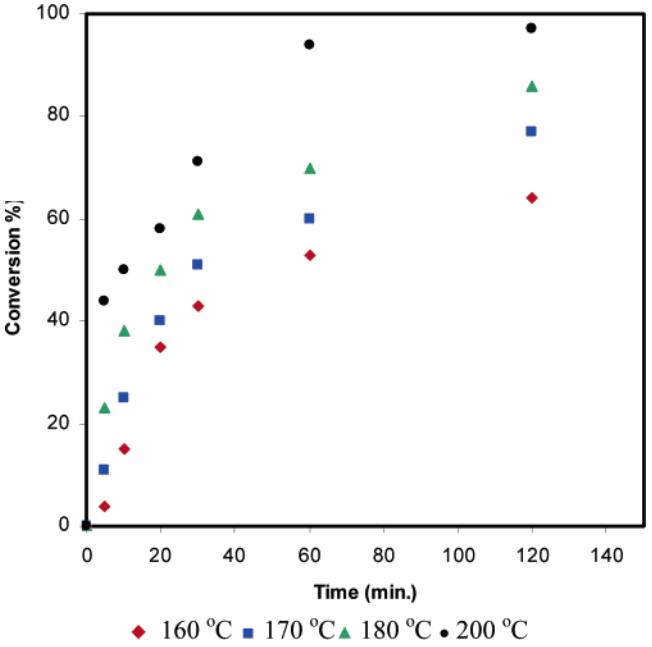

Figure 6. Effect of temperature on cracking of IPA: *m*-cresol = 0.33 mol; IPA = 0.066 mol; UDCaT-5 = 0.05 g cm^{-3}; speed of agitation = 1000 rpm; total volume = 35 cm^3.

propylene. This mole ratio was unfavorable. The rate of alkylation of *m*-cresol was faster at mole ratio of 5:1 with good conversion of IPA. Thus all the subsequent reactions were carried out with a mole ratio of 5:1. The propylene formed was less at this mole ratio, and it was immediately used for alkylation reaction, and hence no isopropyl-*m*-cresol ether was observed for this mole ratio. The decrease in selectivity for the ether with an increase in mole ratio of *m*-cresol to isopropyl alcohol may be because with an increase in amount of *m*-cresol, the rate of intramolecular rearrangement of isopropyl-*m*-cresol ether to the C-alkylated product increases. A mole ratio of 5:1 was maintained (i) to avoid the formation of large amounts of secondary products, such as the oligomers of propylene and dialkylated products and (ii) to diminish the influence of the water formed by the dehydration of IPA in situ. The reaction was also carried out with *m*-cresol to IPA mole ratio 1:5. Even though the conversion of isopropyl alcohol was significant, the rate of alkylation of *m*-cresol with propylene formed was very slow under the same reaction conditions. Also the products formed mainly were DIPE and the O-alkylated product.

3.7. Effect of Temperature. Intrinsically kinetically controlled reactions show significant increase in the conversion profile with temperature. Since almost all mass transfer limitations were eliminated, the effect of temperature was studied on two reaction steps.

3.7.1. Dehydration of IPA. IPA dehydration reaction was studied in the temperature range of 433−473 K. Propylene and diisopropyl ether were the products formed. The rate of dehydration increased with increase in temperature as shown in Figure 6. The product distribution is shown in Figure 7. It was found that the formation of DIPE increased sharply with temperature. Since propylene is difficult to sample and quantify, the concentrations of isopropyl alcohol and isopropyl ether were first quantified by GC and then a mass balance was established to calculate the concentrate of propylene.

3.7.2. Alkylation of m-Cresol with IPA. Figures 8 and 9 show the effect of temperature on the conversion and selectivity of the isopropylation reaction with IPA as the alkylating agent. The rate of reaction increased with increase in temperature, and

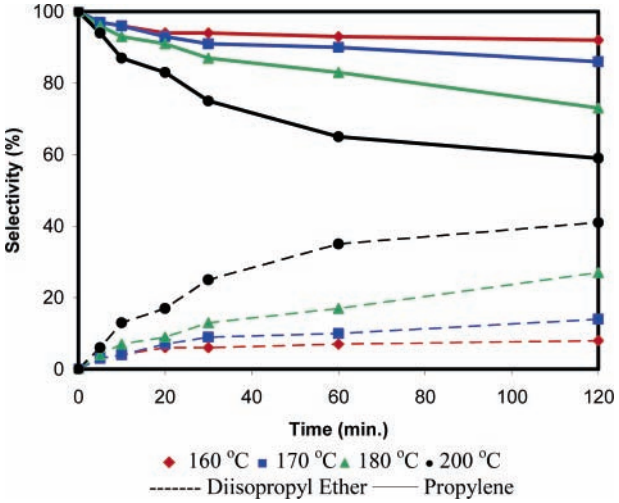

Figure 7. Effect of temperature on selectivity in dehydration of IPA: *m*-cresol = 0.33 mol; IPA = 0.066 mol; UDCaT-5 = 0.05 g cm^{-3}; speed of agitation = 1000 rpm; total volume = 35 cm^3.

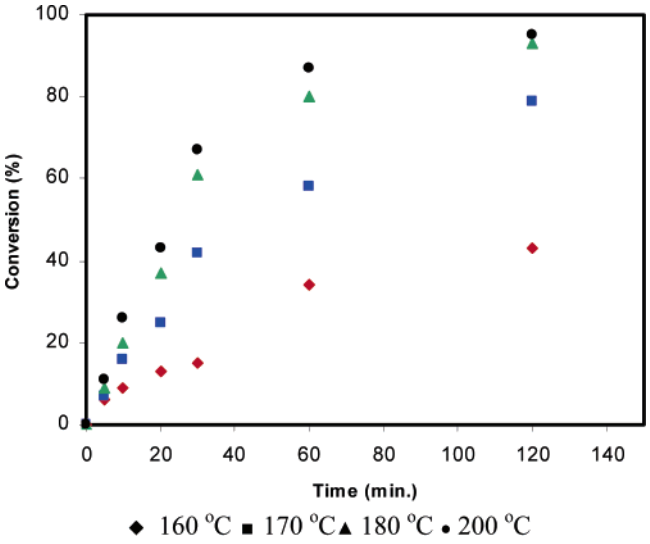

Figure 8. Effect of temperature on alkylation of *m*-cresol with IPA: *m*-cresol = 0.33 mol; IPA = 0.066 mol; UDCaT-5 = 0.05 g cm^{-3}; speed of agitation = 1000 rpm; total volume = 35 cm^3.

selectivity for the thymol was also increased. The selectivity toward the isopropyl-*m*-cresol ether dropped marginally from 32% at 180 °C to 16% at 200 °C for the same conversion level (61%). Thus it shows that the O-alkylation requires the less activation energy than C-alkylation. This decrease in isopropyl-*m*-cresol ether selectivity is due the commonly observed acid-catalyzed rearrangement of alkyl aryl ethers.

3.8. Reaction Kinetics. The process of isopropyl alcohol dehydration to propylene involves the adsorption of the alcohol through the OH group and a β-hydrogen, the abstraction of the OH group to produce an intermediate carbocation species, and the abstraction of the β-hydrogen to yield the olefin.[42,43] The chemisorption of isopropyl alcohol at 40 °C (even room temperature) leads to the coverage of the catalysts with a monolayer of adsorbed isopropoxy species and avoids surface reaction. Strong Brönsted (H^+) and Lewis acid sites catalyze the dehydration of isopropyl alcohol to propylene and diisopropyl ether (on weak Lewis acid sites).[44,45] Indeed, as pointed out by Grambero and Briand,[45] isopropyl alcohol chemisorption and temperature-programmed surface reaction spectroscopy are used to determine the nature, number, and acid strength of the surface/bulk active sites of solid acids. On solid acids such as

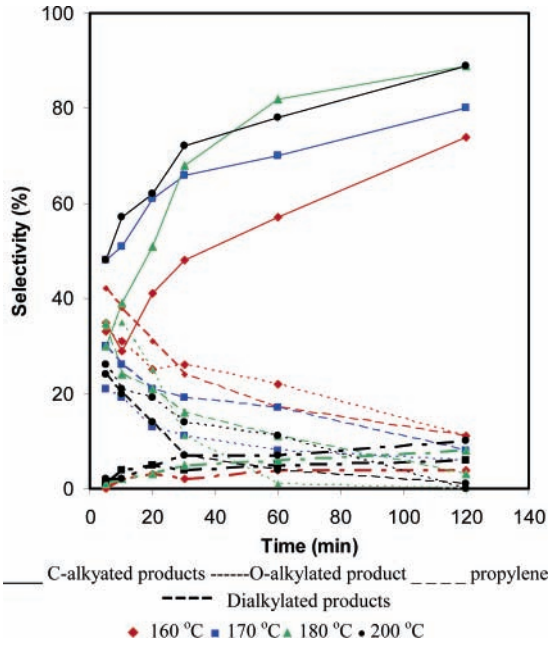

Figure 9. Effect of temperature on selectivity of products: *m*-cresol = 0.33 mol; IPA = 0.066 mol; UDCaT-5 = 0.05 g cm^{-3}; speed of agitation = 1000 rpm; total volume = 35 cm^3.

totally dehydrated $H_3PW_{12}O_{40}$ and $H_6P_2W_{18}O_{62}$, which are very strong acids, there was no isopropyl alcohol adsorption at 96 °C, whereas there was weak adsorption on totally hydrated heteropolyacids. The degree of hydration of the heteropolyanions greatly modifies the amount of accessible sites for isopropyl alcohol adsorption and further dehydration on heteropolyacids. However, it does not influence the catalytic activity of the sites since the temperature of surface reaction of the isopropoxy species is about 96 °C regardless of the degree of hydration.[45] The dehydration of IPA over solid superacids leads to propylene and also diisopropyl ether, which we have earlier studied independently over a number of solid acids including sulfated zirconia and heteropolyacids supported on clay. All our catalysts are superacids that are based on zirconia and the reaction temperature was 180 °C. Solid superacids have both Lewis and Bronsted sites, and thus the mechanism involves bifunctional sites S_1 and S_2. We have recently reported alkylation of several substituted aromatics using linear and branched alcohols and ethers using a variety of solid acid catalysts, wherein a free olefin and water are generated along with the C- or O-alkylated products or both.[22,36,46−51] In a condensation reaction of two alcohols, it was found that symmetrical or asymmetrical ethers are formed (e.g., MTBE from methanol and *tert*-butyl alcohol) in which sulfated zirconia, ion-exchange resin, and 20% w/w $Cs_{2.5}H_{0.5}PW_{12}O_{40}$/K-10 clay were employed as catalysts. With isopropyl alcohol as an alkylating agent, the formation of diisopropyl ether could be witnessed depending on reaction conditions and type of catalysts. Furthermore when *m*-cresol was reacted with IPA over UDCaT-4, the reaction was found to follow second order. Thus, it is seen that the alkylation with alcohols does not follow a simple reaction pathway and our current rate data needed testing of different hypotheses. Several models were tried to fit the experimental data, which were collected in the absence of any external mass transfer and intraparticle diffusion limitations.

The dehydration of IPA to propylene is remarkably dependent on the temperature and was studied independently on UDCaT-4,[33] which is a superacid. It is found that the conversion of IPA increases substantially with increasing temperature at high space time. It was observed that no diisopropyl ether was formed above 150 °C, and thus to elucidate the effect of the temperature and space velocity on selectivity toward propylene and diisopropyl ether a temperature range 110−150 °C was selected, and DIPE was formed in significant quantities in this range. Selectivity toward propylene was also found to be dependent on temperature and space velocity, and it increases with increasing temperature and space velocity.. There was no coking in the temperature range covered in this work. The foregoing results suggested that the dehydration of isopropyl alcohol to propylene and water must proceed via formation of diisopropyl ether. Thus to understand the exact mechanism of dehydration, the cracking diisopropyl ether was studied independently under otherwise similar conditions as the dehydration of isopropyl alcohol in the range of 110−150 °C. The conversion of DIPE and selectivity toward propylene and isopropyl alcohol were found to depend on the temperature and space time. Both the conversion of DIPE and selectivity toward propylene increase substantially with increasing temperature and space velocity. This further corroborates that dehydration of isopropyl alcohol proceeds via formation of diisopropyl ether, which is instantaneously cracked into propylene and water. The dehydration of IPA was found to obey an overall second-order kinetics contrary to the expected first-order kinetics for weakly adsorbed species.[33] Further, it was found that the alkylation of *m*-cresol also followed a second-order reaction. Thus mechanistic models were needed to describe IPA dehydration to propylene and DIPE and alkylation of *m*-cresol. These two cases are considered here, (i) dehydration of IPA to propylene and water and (ii) alkylation of *m*-cresol.

3.8.1. IPA Dehydration.

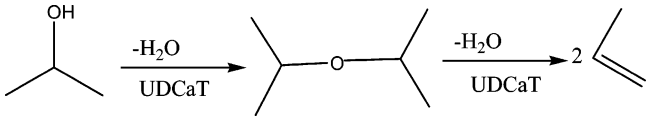

The analysis of earlier published reports on the dehydration of isopropyl alcohol suggests that there is a production of ether and also two types of sites should be involved in the reaction. Thus, a model based on two catalytic sites was proposed according to which IPA (A) gets adsorbed onto two different sites S_1 and S_2. These two adsorbed species participate in the reaction. Assuming that the rate-determining step is the reaction of AS_1 and AS_2 to form diisopropyl ether and water as the surface complexes (ES_1) and (WS_2), respectively, and ES_1 subsequently decomposes instantly into propylene (P), we get

$$A + S_1 \overset{K_{1-A}}{\longleftrightarrow} AS_1 \quad (1)$$

$$A + S_2 \overset{K_{2-A}}{\longleftrightarrow} AS_2 \quad (2)$$

$$AS_1 + AS_2 \overset{K_{SR_1}}{\longleftrightarrow} ES_1 + WS_2 \quad (3)$$

$$ES_1 \overset{K_{SR_2}}{\longleftrightarrow} 2P + WS_1 \quad (4)$$

The site balance in this case is

$$C_{T-S_1} = C_{V-S_1} + C_{A-S_1} + C_{E-S_1} + C_{W-S_1} \quad (5a)$$

$$C_{T-S_2} = C_{V-S_2} + C_{A-S_2} + C_{W-S_2} \quad (5b)$$

The following adsorption equilibria for different species hold

$$W + S_1 \overset{K_{1-W}}{\longleftrightarrow} WS_1 \quad (6a)$$

$$W + S_2 \overset{K_{2-W}}{\longleftrightarrow} WS_2 \quad (6b)$$

$$E + S_1 \overset{K_{1-E}}{\longleftrightarrow} ES_1 \quad (6c)$$

Thus the rate of formation of propylene is

$$-r_p = \frac{k_{SR_1} K_{1-A} C_A K_{2-A} C_A C_{T-S_1} C_{T-S_2}}{(1 + K_{1-A} C_A + K_{1-W} C_W + K_{1-E} C_E)(1 + K_{2-A} C_A + K_{2-W} C_W} \quad (7)$$

When the adsorption constants of all species are very weak, eq 7 is reduced to

$$-r_p = k_p w C_A^2 \quad (8)$$

where

$$k_p = k_{SR_1} K_{1-A} K_{2-A} C_{T-S_1} C_{T-S_2} \quad (9)$$

Writing in terms of conversion and further integration results into

$$\frac{X_A}{1 - X_A} = k w C_{A_0} t$$

Thus a plot of $X_A/(1 - X_A)$ against t (Figure 11) was made to get an excellent fit thereby supporting the model. This is an overall second-order reaction for weak adsorption of IPA.

3.8.2. Isopropylation of m-Cresol.

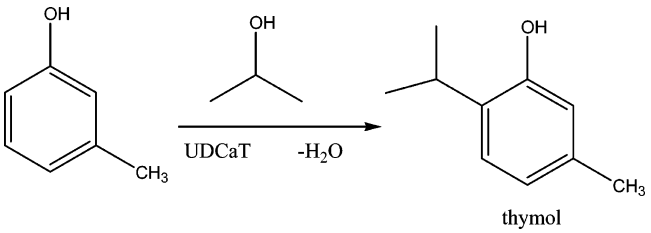

As is validated above, IPA dehydration follows second-order kinetics by adsorption of IPA on two adjacent sites, S_1 and S_2, and the product ether (E) is formed, which is decomposed instantaneously to propylene (P). We have also reported earlier[33,36] the dehydration of IPA over a broad range of temperature (110−150 and 180−220 °C). It has been shown that the rate of alkylation is not controlled by the dehydration rate. Thus in the temperature range studied, the rate of alkylation is not controlled by the dehydration rate but by alkylation of *m*-cresol adsorbed on site S_2 with IPA adsorbed on adjacent site S_1 as shown below.

$$BS_2 + AS_1 \xrightarrow{k_{SR_2}} DS_2 + WS_1 \quad (10)$$

Analogously, the site balance can be written to obtain

$$-r_A = \frac{k_{SR_2} C_{T-S_1} C_{T-S_2} K_{1-A} C_A K_{2-B} C_B}{(1 + K_{1-A} C_A + K_{1-W} C_W + K_{1-E} C_E)(1 + K_{Z-B} C_B + K_{Z-D} C_D)} \quad (11)$$

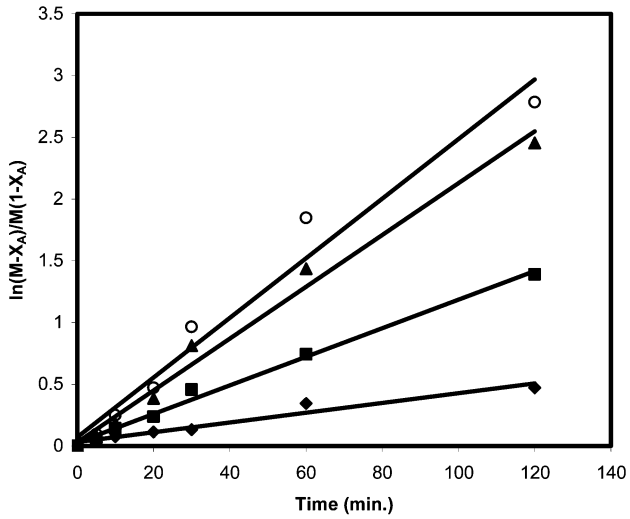

◆ 160 °C ■ 170 °C▲ 180 °C • 200 °C

Figure 10. Validation of mathematical model for isopropylation of *m*-cresol with IPA.

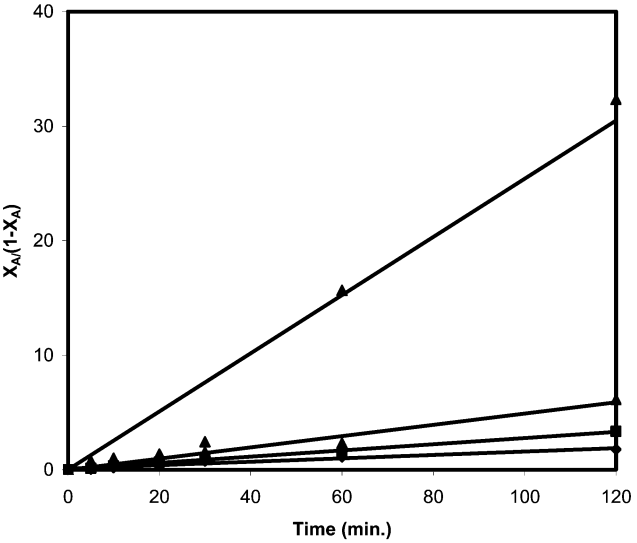

◆ 160 °C ■ 170 °C▲ 180 °C • 200 °C

Figure 11. Validation of mathematical model for dehydration of IPA.

With weak adsorption of all species, it gives the following

$$-r_A = k_A w C_A C_B \quad (12)$$

where

$$k_A = k_{SR_2} C_{T-S_1} C_{T-S_2} K_{1-A} K_{2-B} \quad (13)$$

Writing in terms of conversion and further integration results in

$$\ln\left[\frac{M - X_A}{M(1 - X_A)}\right] = (M - 1) k_A C_{A_0} t \quad (14)$$

Thus, a plot of $\ln[M - X_A/(M(1 - X_A))]$ against t is shown in Figure 10. It is seen that the data fit very well. The values of rate constants at different temperatures were calculated and an Arrhenius plot (Figure 12) was used to estimate activation energy. The value of the activation energy was calculated as 32.25 kcal mol^{-1}. This activation energy also supported the fact that the overall rate of reaction is not influenced by either

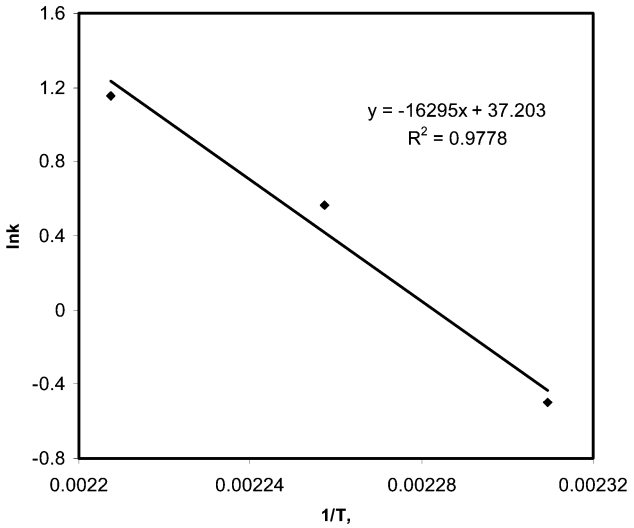

Figure 12. Arrhenius plot of ln k vs $1/T$ (in K^{-1}).

external mass transfer or intraparticle diffusion resistance, and it is an intrinsically kinetically controlled reaction on active sites.

3.9. Reusability of Catalyst. Reusability of UDCaT-5 was verified by conducting two runs. After each run, the catalyst was filtered, washed with IPA, dried at 120 °C for 2 h, and weighed before using in the next batch. There was some attrition of catalyst particle during agitation. In a typical batch reaction, there were inevitably losses of particles during filtration due to attrition. Although the catalyst was washed after filtration to remove all adsorbed reactants and products, there was still a possibility of retention of a small amount adsorbed reactants and product species, which might cause the blockage of active sites of the catalyst. These are apparent factors for the loss in activity, which have been taken into account because no fresh catalyst was added into the reaction mixture to maintain the same catalyst loading during reusability tests. The actual amount of catalyst used in the next batch was almost 5% less than the previous batch. It was observed that there is only a marginal decrease in conversion. When makeup quantity of the catalyst was added, almost similar conversions were found to suggest that the catalyst is stable.

4. Conclusion

Liquid-phase isopropylation of *m*-cresol with isopropyl alcohol as an alkylating agent was examined by using various modified versions of zirconia. UDCaT-5 was found to be the best catalyst in terms of activity and selectivity. The rate of reaction increased with temperature, catalyst loading, and *m*-cresol/isopropyl alcohol ratio. The reaction condition should be carried out at 180 °C with catalyst loading of 0.05 g cm^{-3} with mole ratio of *m*-cresol/isopropyl alcohol 5:1 to obtain thymol with maximum yield. We believe that this is a novel method to synthesize thymol at a low temperature and with high activity and selectivity using superacidic UDCaT-5 catalyst. This method can be a replacement for the commercial method of thymol production. Comprehensive mathematical models were developed and validated with experimental results. The second order kinetics fits the data well, and the activation energy was found to be 32.25 kcal mol^{-1}. The conditions are optimized in a way to get thymol selectively at low temperature. The reaction is solvent-free, which could be advantageous as a green process.

Acknowledgment. G.D.Y. acknowledges support from the Darbari Seth Endowment for the Chair. A Junior Research Fellowship (JRF) by the Council of Science and Industrial Research (CSIR), Government of India, New Delhi, was awarded to G.S.P.

Nomenclature

A = reactant species A, IPA
B = reactant species B, *m*-cresol
C = O-alkylated product
D = thymol
C_A = Concentration of A, kmol m^{-3}
C_{A_0} = initial concentration of A at solid (catalyst) surface, kmol m^{-3}
C_B = concentration of B, kmol m^{-3}
C_{V-S_i} = concentration of vacant sites of type *i* (1 or 2), kmol m^{-3}
E = Diisopropyl ether
K_{SR_i} = surface reaction equilibrium constant for reaction *i*, k_{SR_i}/k'_{SR_i}
k_{SR_i} = surface reaction rate constant for forward reaction *i*
k'_{SR_i} = surface reaction rate constant for reverse reaction *i*
k_A = overall second order rate constant for A with B, cm^6 mol^{-1} g^{-1} s^{-1}
k_P = overall second order rate constant for dehydration of IPA (P), cm^6 mol^{-1} g^{-1} s^{-1}
M = mole ratio
$-r_B$ = rate of reaction of B with A, mol cm^{-3} s^{-1}
r_i = overall rate of reaction of species *i* per unit liquid phase volume, mol cm^{-3} s^{-1}
w = catalyst loading per unit liquid volume, g cm^{-3}
X_A = fractional conversion of A

Subscripts
S = vacant site
SR = surface reaction
i−j = type of site i where species j is adsorbed
$T-S_i$ = total sites S of type i
V−Si = vacant sites S of type i
W = water
X_A = fractional conversion of A

References and Notes

(1) Olah, G. A. *Friedel-Craft and Related Reactions*; Wiley Interscience: New York and London, 1963; Vols. 1−4.
(2) Olah, G. A.; Krishanamuri, R.; Surya Prakash, G. K. *Comprehensive Organic Synthesis*; Pergamon: Oxford, U.K., 1991; Vol. 3, Chapter 1.8.
(3) Clark, J. H.; Macquarrie, D. J. *Org. Process Res. Dev.* **1997**, *1*, 149.
(4) Corma, C.; Garcia, H. *Chem. Rev.* **2003**, *103*, 4307.
(5) Corma, A. *Chem. Rev.* **1995**, *95*, 559.
(6) *Ullmann's Encyclopedia of Industrial Chemistry*; Wiley-VCH Verlag GmbH: Weinheim, Germany, 2002.
(7) Nitta, M. *Bull. Chem. Soc. Jpn.* **1974**, *47*, 2360.
(8) Stroh, R.; Seydel, R.; Hahn, W. *Newer Methods of Preparative Organic Chemistry*; Academic Press: New York, 1963; Vol. 2, p 337.
(9) Umamaheswari, V.; Palanichamy, M.; Murugesan, V. *J. Catal.* **2002**, *210*, 367.
(10) Teissedre, P. L.; Waterhouse, A. L. *J. Agric. Food Chem.* **2000**, *48*, 3801.
(11) Krause, E. L.; Ternes, W. *Eur. Food Res. Technol.* **1999**, *209*, 140.
(12) Yanishlieva, N. V.; Marinova, E. M.; Gordon, M. H.; Raneva, V. G. *Food Chem.* **1999**, *64*, 59.
(13) Milos, M.; Mastelic, J.; Jerkovic, I. *Food Chem.* **2000**, *71*, 79.
(14) Grabowska, H.; Wrzyszcz, *J. Res. Chem. Intermed.* **2001**, *27*, 281.
(15) Velu, S.; Sivasanker, S. *J. Res. Chem. Intermed.* **1998**, *24*, 657.
(16) Yamanaka, T. *Bull. Chem. Soc. Jpn.* **1976**, *49*, 2669.
(17) Franc, H. G.; Stadelhofer, J. W. *Industrial Aromatic Chemistry*; Springer-Verlag: Berlin/Heidelberg, 1998; p 168.
(18) Biedarmann, W.; Koller, H.; Wedemeyer, K. U.S. Patent 4,086,-283, 1978.
(19) Wimmer, P.; Buysch, H. J.; Puppe, L. U.S. Patent 5,030,770 1991.
(20) Klein, A.; Wedemeyer, K. Bayer DE-OS 2242628, 1972.
(21) Yadav, G. D.; Nair, J. J. *Microporous Mesoporous Mater.* **1999**, *33*, 1.

(22) Yadav, G. D.; Salgaokar, S. S. *Ind. Eng. Chem. Res.* **2005**, *44*, 1706−1715.
(23) Knozinger, H.; Ratnasamy, P. *Catal. Rev. Sci. Eng*. **1978**, *17*, 31.
(24) Balaceanu, J. C.; Jungers, J. C. *Bull. Soc. Chim. Belg.* **1961**, *60*, 476.
(25) Knozinger, H.; Kallo, D. *Chem. Eng. Technol.* **1967**, *39*, 676.
(26) Jain, J. R.; Pillai, C. N. *J. Catal*. **1967**, *9*, 322.
(27) Santacesaria, E.; Gelosa, O.; Giorgi, E.; Carrb, S. *J. Catal*. **1984**, *90*, 1.
(28) Davis, B. H. In *Adsorption and catalysis on oxide surfaces*; Che, M., Bond, G. C., Eds.; Elsevier: Amsterdam, 1985; p 309.
(29) Golay, S.; Doepper, R.; Renken, A. *Chem. Eng. Sci*. **1999**, *54*, 4469−4474.
(30) Lou, J. C.; Parera, J. M. *Appl. Catal.* **1986**, *26*, 295−305.
(31) Yadav G. D.; Thorat, T. S. *Ind. Eng. Chem. Res.* **1996**, *35* (3), 721−732.
(32) Yadav, G. D.; Manyar, H. G. *Microporous Mesoporous Mater*. **2003**, *63* (1−2), 85−96.
(33) Yadav, G. D.; Murkute, A. D. *Langmuir* **2004**, *20* (26), 11606−11619.
(34) Yadav, G. D.; Murkute, A. D. *J. Catal*. **2004**, *224*, 218.
(35) Yadav, G. D.; Murkute, A. D. *J. Phys. Chem. A* **2004**, *108* (44), 9557−9566.
(36) Yadav, G. D.; Salgaokar, S. S. *Microporous Mesoporous Mater*. **2005**, *80*, 129.
(37) Yadav, G. D.; Asthana, N. S. *Appl. Catal. A: Gen*. **2003**, *244*, 341−357.
(38) Yadav, G. D.; Asthana, N. S.; Kamble, V. S. *Appl. Catal. A: Gen*. **2003**, *240*, 53−69.
(39) Yadav, G. D.; Salgaonkar, S. S.; Asthana, N. S. *Appl. Catal. A: Gen*. **2004**, *265*, 153−159.
(40) Yadav, G. D.; Asthana, N. S.; Kamble, V. S. *J. Catal*. **2003**, *217* (1), 88−99.
(41) Fogler, S. H. *Elements of Chemical Reaction Engineering*, 2nd ed.; Prentice-Hall: New Delhi, 1995, pp 625−626.
(42) Gervasini, A.; Fenyvesi, J.; Auroux, A. *Catal. Lett*. **1997**, *43*, 219.
(43) Youssef, A. M.; Khalil, L. B.; Girgis, B. S. *Appl. Catal.* **1992**, *81*, 1.
(44) Larsen, G.; Lotero, E.; Petkovic, L. P.; Shobe, D. *J. Catal*. **1997**, *169*, 6.
(45) Gambaro, L. A.; Briand L. E. *Appl. Catal. A: Gen.* **2004**, *264*, 151−159.
(46) Yadav, G. D.; Doshi, N. S. *Appl. Catal. A.: Gen*. **2002**, *236* (1−2), 129−147.
(47) Yadav, G. D.; Doshi, N. S. *J. Mol. Catal. A: Chem.* **2003**, *194* (1−2), 195−209.
(48) Yadav, G. D.; Kirthivasan, N. *J. Chem. Soc., Chem. Commun.* **1995**, 203−204.
(49) Yadav, G. D.; Bokade, V. V. *Appl. Catal. A: Gen*. **1996**, *147* (2), 299−315.
(50) Yadav, G. D.; Kirthivasan, N. In *Fundamental and Applied Aspects of Chemically Modified Surfaces*; Blitz, J. P., Little, C. B., Eds.; Royal Society of Chemistry: Cambridge, U.K., 1999; pp 254−269.
(51) Yadav, G. D.; Joshi, A. V. *Org. Process Res. Dev*. **2001**, *5*, 408−414.